Ligand Modulation of Lateral Segregation of a G-Protein-Coupled Receptor into Lipid Microdomains in Sphingomyelin/Phosphatidylcholine Solid-Supported Bilayers†

Isabel D. Alves,‡ Zdzislaw Salamon,§ Victor J. Hruby,‡,§ and Gordon Tollin*,‡,§

Department of Chemistry and Department of Biochemistry and Molecular Biophysics, University of Arizona, Tucson, Arizona 85721

Received February 3, 2005; Revised Manuscript Received April 19, 2005

ABSTRACT: A growing body of evidence supports the idea that the plasma membrane bilayer is characterized by a laterally inhomogeneous mixture of lipids, having an organized structure in which lipid molecules segregate into small domains or patches. Such microdomains are characterized by high contents of sphingolipids that form thicker liquid-ordered regions that are resistant to extraction with nonionic detergents. The existence of lipid lateral segregation has been demonstrated in both model and biological membranes, although its role in protein sorting and membrane function still remains unclear. In these studies, plasmon-waveguide resonance (PWR) spectroscopy was employed to investigate the properties of microdomains in a model system consisting of a solid-supported lipid bilayer composed of a 1:1 mixture of palmitoyloleoylphosphatidylcholine (POPC) and brain sphingomyelin (SM), and their influence on the partitioning and functioning of the human delta opioid receptor (hDOR), a G-protein coupled receptor (GPCR). Resonance signals corresponding to two microdomains (POPC-rich and SM-rich) were observed in such bilayers, and the sorting of the receptor into each domain was highly dependent on the type of ligand that was bound. When no ligand was bound, the receptor was incorporated preferentially into the POPC-rich domain; when an agonist or antagonist was bound, the receptor was incorporated preferentially into the SM-rich component, although with a 2-fold greater propensity for this microdomain in the case of the agonist. Binding of G-protein to the agonist-bound receptor in the SM-rich domain occurred with a 30-fold higher affinity than binding to the receptor in the PC-rich domain. The binding of the agonist to an unliganded receptor in the bilayer produced receptor trafficking from the PC-rich to the SM-rich component. Since the SM-rich domain is thicker than the PC-rich domain, and previous studies with the hDOR have shown that the receptor is elongated upon agonist activation, we propose that hydrophobic matching between the receptor and the lipid is a driving force for receptor trafficking to the SM-rich component.

For the past three decades, the fluid mosaic model of Singer and Nicholson (*1*) has provided the foundation for the understanding of membrane structure. According to this model, membranes are viewed as laterally homogeneous lipid assemblies where the bilayer functions as a noninteracting two-dimensional solvent, having little influence on membrane protein function. During the past decade, evidence indicating that lateral segregation into lipid microdomains occurs in membranes has accumulated (see ref *2* for a review). Microdomain formation occurs by spontaneous aggregation of certain naturally occurring lipids that spontaneously aggregate in the plane of the membrane, which is driven solely by distinctive intermolecular interactions, including van der Waals forces between the long, largely saturated chains of sphingomyelin and glycosphingolipids, as well as hydrogen bonding between adjacent glycosyl moieties (*3*). Operationally, lipid laterally segregated microdomains have been defined by their insolubility in nonionic detergents at 4 °C, and by a light buoyant density on sucrose gradients (*3*, *4*). Microdomains are also characterized by a higher degree of molecular order (induced by the presence of saturated fatty acyl chains and sometimes cholesterol), and by being thicker than the surrounding liquid-disordered lipids in the membrane.

Different methodologies have been used to investigate lipid microdomains, both in vivo and employing model membranes, such as nonionic detergent extraction at low temperatures, cholesterol depletion, and direct observation by different microscopic and spectroscopic methods (AFM,[1] FRET, FRAP, FCS, SPT, etc.; see refs *3* and *5* for reviews). Depending on the method employed and whether model membranes or cells were studied, results for the size, lifetime, and composition of microdomains are diverse and controversial. Apart from these controversies, there is common agreement about the existence of microdomains in model

† This work was supported by grants from the Vice President for Research, University of Arizona (to G.T. and V.J.H.), the National Institutes of Health (Grant GM59630 to G.T. and Z.S.), the U.S. Public Health Service, and NIDA (Grants DA-06284 and DA13449 to V.J.H.).

* To whom correspondence should be addressed: Department of Biochemistry and Molecular Biophysics, University of Arizona, 1041 E. Lowell St., Tucson, AZ 85721. Phone: (520) 621-3447. Fax: (520) 621-9288. E-mail: gtollin@u.arizona.edu.

‡ Department of Chemistry.

§ Department of Biochemistry and Molecular Biophysics.

10.1021/bi050207a CCC: $30.25
Published on Web 06/01/2005

membranes that form spontaneously in mixtures of SM and unsaturated phospholipids such as DOPC and POPC, in both the presence and absence of cholesterol (*2*).

One of the most important roles of lipid microdomains at the cell surface may be their function in signal transduction. Given the overall low abundance of key signaling molecules in cells, one way to account for the rapid response characteristic of signal transduction is that cells concentrate signaling molecules in membrane microdomains. Such domains could be viewed as platforms that serve to localize the requisite components, facilitating their interaction and supporting signaling. In this view, a given receptor and its effector molecules would be localized in a single microdomain. Activation by the hormone signal would lead to a rapid and efficient signal transduction due to the proximity of the interacting partners. The specificity of the signaling could be enhanced by restricting the receptor to a particular domain containing a different subset of signaling partners. In another view, complementary components of a signaling pathway would be segregated into different domains under basal conditions, and following activation, those components could be joined by domain fusion. Alternatively, domains could contain nearly complete signaling pathways that would be activated when a receptor or another molecule is recruited into the microdomain, promoting interaction and leading to signaling. Microdomains could provide more specificity and diversity in the signaling cascade by providing compartmentalization to the different components that are involved or by modulating the intrinsic activities of the proteins located therein. The relative biological importance of these various mechanisms remains to be elucidated.

Under basal conditions, some GPCRs are almost exclusively located in microdomains [e.g., more than 90% of the gonadotrophin-releasing hormone receptor (*6*)], whereas others are present in a small amount [e.g., <10% of the oxytocin receptor (*7*, *8*)]. In other cases, the localization of GPCRs to lipid microdomains is modulated by ligand binding (for reviews, see refs *9* and *10*). For the β_2-adrenergic receptor (*11*) and the adenosine A_1 receptor (*12*), treatment with agonist causes translocation of the cognate receptor out of lipid microdomains. By contrast, the angiotensin II type receptor (*13*), the muscarinic receptor (*14*), and the bradykinin B_1 and B_2 receptors (*15*−*17*) are targeted to microdomains upon activation by an agonist. Others such as the endothelin receptor are apparently unaffected by agonist binding (*18*). However, the functional significance of agonist-induced receptor localization has not been demonstrated. It is possible that ligand-induced movement of the receptor into lipid microdomains may promote association of the receptor with G-proteins or effector enzymes that are enriched in this compartment. Since laterally segregated membrane regions are involved in endocytosis, the sequestration of the receptor into those domains may be involved in desensitization via removal from the cell surface.

[1] Abbreviations: AFM, atomic force microscopy; DPDPE, c-[D-Pen^2,D-Pen^5]enkephalin; FCS, fluorescence correlation spectroscopy; FRAP, fluorescence recovery after photobleaching; FRET, fluorescence resonance energy transfer; GPCR, G-protein-coupled receptor; GTPγS, guanosine triphosphate γS; hDOR, human delta opioid receptor; NTI, naltrindole; PC, phosphatidylcholine; polar., polarization; PWR, plasmon-waveguide resonance; SM, sphingomyelin; SPT, single particle tracking.

Another issue is hydrophobic matching involving the length of the transmembrane domains of the protein, because a liquid-ordered bilayer is thicker than a liquid-disordered one. These parameters play a role in the sorting of protein to the cell surface (*19*, *20*). However, how precisely the transmembrane domains need to be matched with the thickness of the bilayer is an open issue. So far, no detailed analysis has been carried out to determine how transmembrane proteins having different transmembrane domain lengths partition into the different domains.

In this work, we have investigated the partitioning of a GPCR [i.e., the human delta opioid receptor (hDOR)] between PC-rich and SM-rich domains in a model system consisting of solid-supported lipid bilayers, and the resulting effects of the microenvironmental differences on G-protein binding affinity and activation. This receptor belongs to family A of the GPCRs and is involved in a plethora of biological events such as analgesia, locomotive activity, blood pressure, gastrointestinal motility, learning, and memory (*21*). We should mention that the hDOR is mainly located in the spinal cord and in the brain, areas whose membranes are very rich in unsaturated lipids and sphingolipids, and thus have the potential for microdomain formation. This receptor has been the subject of interest in our laboratories over the past several years, and we have investigated ligand-induced conformational changes and receptor−G-protein interactions using plasmon-waveguide resonance (PWR) spectroscopy (*22*, *23*).

We have also used PWR spectroscopy to examine solid-supported lipid bilayers consisting of pure lipids (DOPC, POPC, and SM), and PC/SM binary mixtures (*24*). We have shown that a single lipid bilayer formed from the PC/SM mixture consists of microdomains enriched in the SM component, coexisting with PC-rich domains, whose different optical properties allow observation of separate resonances in a PWR experiment. These are formed spontaneously over time as a consequence of lateral phase separation. The uniqueness of the PWR technique is that it allows the mass and structural characteristics of a lipid membrane to be determined for a single bilayer in both steady-state and kinetic modes. Unlike other techniques for domain visualization, PWR can also provide insights into microenvironmental effects on protein functional properties (*23*) in model systems that simulate a natural lipid bilayer. Simulation of the PWR spectra allowed the deconvolution of the complex spectra of the binary mixtures into single resonance spectra corresponding to the two microdomains. Comparison of the spectra of the mixtures with those of the pure lipids has shown that the resonance occurring at smaller angles is due to a microdomain containing mainly PC molecules, with a small admixture of SM (PC-rich component), whereas the higher angle resonance consists predominantly of a microdomain composed of SM molecules, with a small admixture of PC (SM-rich component). The ability to resolve resonances corresponding to these bilayer regions is due to their differing microstructure and optical properties, with the PC areas less well ordered, less tightly packed, and thinner than the SM areas as a consequence of the presence of unsaturated fatty acyl chains.

In this study, the partitioning of the hDOR between the two domains (PC- and SM-rich domains) that form spontaneously in a POPC/SM (1:1) bilayer was directly determined

by comparing the spectral shifts obtained for each resonance upon receptor insertion, and the amount of receptor in each microdomain was quantified by spectral simulation. The partitioning of the receptor between the two domains was found to be highly dependent on the type of ligand that was bound to the receptor. Binding of an agonist to the unliganded receptor in the POPC/SM lipid bilayer resulted in receptor trafficking from the PC-rich to the SM-rich domain. We have also measured the binding affinities of G-protein for each of these receptor populations and have shown that the affinity for the agonist-bound hDOR in the SM-rich domain was 30-fold higher than for the receptor in the PC-rich domain.

EXPERIMENTAL PROCEDURES

Plasmon-Waveguide Resonance (PWR) Spectroscopy. PWR spectra are produced by resonance excitation of conduction electron oscillations (plasmons) by light from a polarized CW laser (He−Ne; wavelength of 632.8 or 543.5 nm) incident on the back surface of a thin metal film (Ag) deposited on a glass prism and coated by a layer of SiO_2 (see refs *25*−*28* for additional information). Spectra were obtained with a Proterion Corp. (Piscataway, NJ) instrument that had a spectral resolution of 1 mdeg. The sample to be analyzed (a lipid bilayer membrane) was immobilized on the resonator surface and placed in contact with an aqueous medium, into which proteins and ligands can be introduced. The deposited analyte molecules change the resonance characteristics of plasmon formation and can thereby be detected and characterized. PWR spectra, corresponding to plots of reflected light intensity versus incident angle, can be excited with light whose electric vector is either parallel or perpendicular to the plane of the resonator surface (s- or p-polarization, respectively). This allows the anisotropy of the two refractive index values (n_s and n_p), as well as the sample thickness (t), to be determined, thus providing information about changes in the mass density, structural asymmetry, and molecular orientation induced by biomolecular interactions occurring at the resonator surface.

PWR Spectral Simulation. The purpose of this procedure is to simulate a PWR spectrum consisting of more than one resonance by a superposition of single-resonance curves that have been obtained from bilayers composed of single-lipid components (see ref *24* for details). The simulation has been done in two steps. First, the single-component bilayer spectra were fitted by theoretical resonance curves obtained from Maxwell's equations applied to thin films, which provide an analytical relationship between the experimental spectral parameters and the optical properties of the bilayer (refractive index, n, extinction coefficient, k, and thickness, t). This allows evaluation of the optical parameters, with an error estimated to be about ±3% (see also refs *22*, *25*, *26*, and *28*). In the second step, the complex spectrum obtained from the bilayer formed from binary lipid mixtures was deconvoluted into a sum of single-component spectra. This deconvolution process starts with the single-resonance optical parameters that resulted from the first step, and incorporates variation of these parameters into a final fit of the complex spectrum. It is important to note that the same set of optical parameters will result in a different spectrum if applied to a different PWR sensor. This is why for different sensors there will be differences in spectra even for the same (or very similar) lipid membranes. The simulation process provides information about how much the single-component resonance is modified in the binary lipid mixture, and also about the ratio of the bilayer surfaces that are covered by the different kinds of membrane microdomains exposed to the laser excitation beam.

In this case, the spectra of membranes formed from a single lipid (i.e., POPC and SM) were used as a starting point for spectral simulation of membranes consisting of mixtures of these components. These single-component PWR spectra are distinctively different in both their position and shape due to differences in the optical properties of the bilayer membrane, which are determined by the surface mass density (i.e., mass per unit surface area), the mass distribution (i.e., the internal structure of the membrane, including the molecular anisotropy and the long-range molecular order of the bilayer), the membrane thickness, and the absorption or light scattering properties of the membrane at the plasmon excitation wavelength.

As we will demonstrate below, the PWR spectra of such binary lipid mixtures consist of the superposition of resonances corresponding to two lipid microdomains (POPC-rich and SM-rich) coexisting within the bilayer membrane. Iteration of such simulation was performed by variation of the optical parameters of the appropriate single-lipid component spectrum until satisfactory agreement with the experimental spectra was obtained. The final deconvoluted component spectra that describe the separate microdomains were slightly different from those of the single-component curves, indicating that each of the separate phases contained small amounts of the other lipid. Spectral simulation has also been used to determine the mass density of lipid bilayers containing incorporated protein molecules, thereby allowing the evaluation of the sorting of such proteins into the separate microdomains.

Receptor Purification and Characterization. A fully functional hDOR, labeled at the C-terminus with a *myc* epitope and His tag, was stably transfected into a Chinese hamster ovary cell line (CHO-K1) and the modified receptor purified by metal chelating and ligand affinity chromatography and characterized (*29*, *30*). For the studies in which the receptor was prebound with ligand, the hDOR was preincubated with saturating amounts (a concentration at least 1 order of magnitude higher than published binding affinities) of ligand, using a peptide agonist, DPDPE (American Peptide Co.), a nonpeptide agonist, SNC80 (Tocris Inc., Elisville, MO), and an antagonist, NTI (Sigma). The receptor was incubated with the respective ligand for 1−2 h at 4 °C prior to incorporation into the PWR cell that contained a previously deposited lipid bilayer on the resonator surface. The concentration of the solubilized receptor was determined using a BCA (bicinchoninic acid) assay (Pierce). The purple reaction product was monitored at 560 nm using an ELISA plate reader (μ Quant, Bio-Tek Instruments, Inc.). Following purification, the quality of the receptor protein was assessed by determining the specific activity, i.e., the number of moles of functional receptor molecules (measured by ligand binding) per mole of receptor protein. This was performed by a radiolabel competition assay using [^{3}H]naltrindole (Perkin-Elmer) to a final concentration of ~0.1 nM DPDPE with concentrations ranging from 10^{-3} to 10^{-9} M. Details of the methodology have been previously published (*30*).

Lipid Bilayer Formation. A solid-supported lipid membrane was assembled as previously described (*22*, *25*), using the same principles that govern the spontaneous formation of a freely suspended lipid bilayer membrane across a small orifice in a Teflon sheet that separates two aqueous compartments, the so-called black lipid membrane (*31*). Such a bilayer is anchored to the orifice by an annulus of lipid solution (the Gibbs border) that allows lipid molecules to move into and out of the bilayer in response to protein insertion and/or conformation changes. The lipid films were formed on the hydrated silica surface of the PWR resonator from the following membrane-forming solutions: 10 mg/mL palmitoyloleoylphosphatidylcholine (POPC) and brain sphingomyelin (SM) (1:1 molar ratio) (Avanti Polar Lipids, Alabaster, AL) in a squalene/butanol mixture (0.1:10, v/v). The buffer solution used in the PWR sample cell was 10 mM Tris-HCl containing 10 mM KCl and 0.5 mM EDTA at pH 7.4 (total cell volume of ~1 mL).

Incorporation of the hDOR by Detergent Dilution and G-Protein Addition. The incorporation of the receptor into the lipid bilayer was accomplished by introducing the detergent-solubilized (30 mM octyl glucoside-containing buffer) hDOR (prebound with the ligand under investigation when noted) into the aqueous compartment under conditions that dilute the detergent to below the critical micelle concentration (cmc), which allows the membrane protein to spontaneously incorporate into the lipid bilayer. We have carried out appropriate control experiments that show that, at the concentrations that were used, octyl glucoside does not perturb the deposited lipid bilayer (not shown). To make sure that all receptor molecules had ligand bound before the receptor was added to the PWR cell sample, we have added that same ligand to the sample compartment at a concentration above the K_D value for that ligand. In these experiments, we have access to only the side of the lipid bilayer facing the aqueous compartment (i.e., no direct access is available to the side of the lipid bilayer facing the silica surface of the prism), and we think that neither the G-protein nor most ligands are able to cross the bilayer. However, because binding to both the G-proteins and ligands can occur after receptor incorporation (processes that are known to occur in opposite faces of the receptor), it appears that the receptor inserts bidirectionally into the lipid bilayer, i.e., with the extracellular side facing both the silica surface and the aqueous compartment. Since we were also interested in studying the ternary complex, i.e., ligand, receptor, and G-protein, we have accomplished this, as we have done previously (*30*), by prebinding the receptor with the ligand before incorporation into the lipid bilayer. In this way, some of the ligand-bound receptors will have their G-protein binding sites accessible to the external aqueous medium. Small aliquots of the G_α-protein subtypes found in brain tissue, where this receptor is found, namely, $G_{o\alpha}$, $G_{i\alpha1}$, $G_{i\alpha2}$, and $G_{i\alpha3}$, and the $\beta\gamma$ subunit complex (a mixture of the different $\beta\gamma$ subtypes present in brain) (Calbiochem) were incrementally added to the equilibrated proteolipid system (1:1 α subunit:$\beta\gamma$ dimer ratio). After saturation had been reached, GTPγS (Sigma) was added and the PWR spectral changes were monitored.

It should also be noted that in these experiments, we do not directly determine the concentrations of the receptor and G-protein in the PWR cell. Affinities are obtained from the PWR spectral changes that occur due to mass increases in the proteolipid system upon incremental addition of G-protein to the cell. Since PWR is only sensitive to the optical properties of material that is deposited on the resonator surface, there is no interference from the material that is in the bulk solution. Furthermore, in titrations with G-proteins or with other ligands added to the sample cell, the amount of material bound is quite small compared to the amount present in the bulk solution, and it is assumed that the bulk material is able to freely diffuse and equilibrate with the membrane. Thus, since the spectral changes are proportional to the amount of G-protein bound to the receptor, plots of spectral shifts versus bulk G-protein (or ligand) concentration allow a direct determination of dissociation constants. In other words, a hyperbolic saturation curve corresponds to a plot of the total G-protein (or ligand) added to the aqueous compartment versus the amount bound, and fitting the experimental data to such a curve provides a value for K_D.

RESULTS AND DISCUSSION

Previous studies from our laboratories have demonstrated the successful reconstitution of the human delta opioid receptor (hDOR) into solid-supported lipid bilayers on the sensor surface of a plasmon-waveguide resonance (PWR) spectrometer (*22*, *30*). In those studies, we have shown that the incorporation of the hDOR into the lipid bilayer produces shifts to higher incident angles in the resonance for both p- and s-polarized light. The increase in the resonance angle has been attributed mainly to an increase in the refractive index (correlated with a mass increase) produced by insertion of the receptor into the bilayer. We have also shown that the receptor can incorporate bidirectionally into the bilayer, i.e., with either the C-terminus or N-terminus facing the aqueous compartment of the PWR cell sample, and that it is uniaxially incorporated into the bilayer with the proper orientation. The first conclusion is based upon the fact that both ligands and G-proteins are able to bind to the incorporated receptor. The latter conclusion is derived from the fact that receptor incorporation produces larger spectral shifts for p-polarization than for s-polarization (indicating refractive index changes in the p-direction, i.e., perpendicular to the plane of the bilayer, that were larger than those for the s-direction), which is a consequence of the anisotropic structure (i.e., cylindrical shape) of the receptor molecules. This demonstrates that the receptor has its long axis oriented perpendicular to the bilayer and the shorter axis parallel to the bilayer.

Incorporation of the Agonist-Bound (DPDPE) hDOR in a POPC/SM (1:1) Bilayer. Figure 1 shows typical PWR spectra obtained with either p-polarized (panels A−C) or s-polarized (panels D−F) exciting light for a solid-supported lipid membrane before (panels A and D, curve 1) and after addition of the detergent-solubilized receptor (~10 nM, final concentration in the sample cell) to the aqueous compartment in the sample cell (panels A and D, curve 2). As the curves labeled 1 show, in both polarization cases the resonance spectrum contains shoulders indicating that more than one resonance is occurring within the experimental angular range. This has been observed previously for both DOPC/SM and POPC/SM bilayers (*24*). This more complex spectrum results from the superposition of two individual resonances, which indicates the presence of lateral phase separation in this lipid

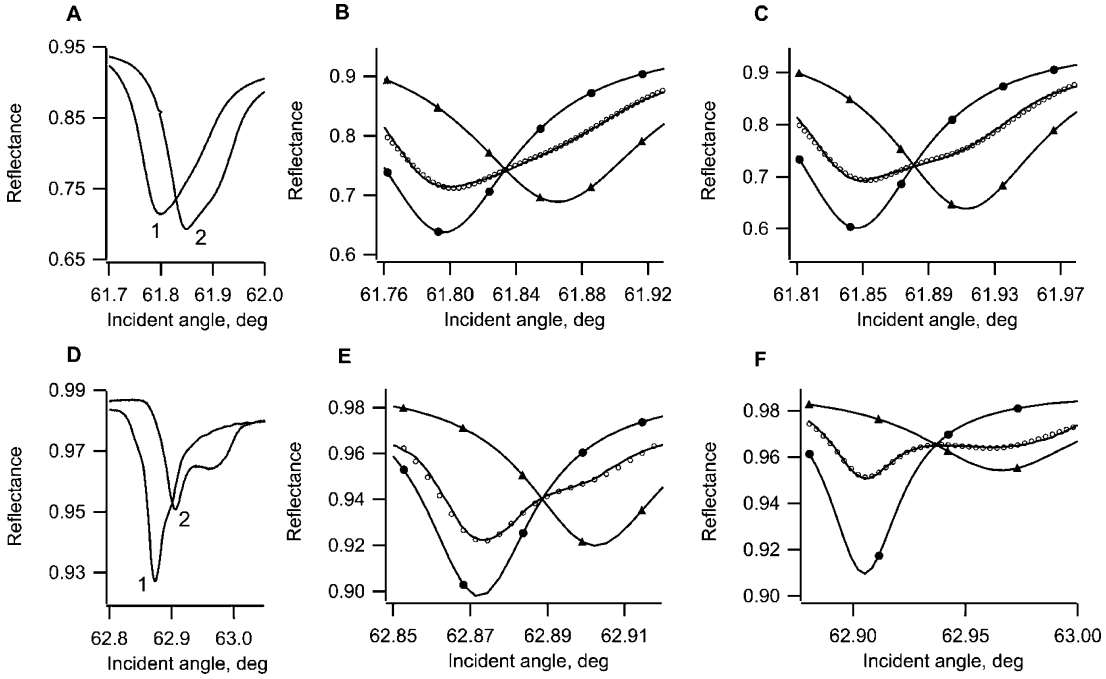

FIGURE 1: PWR spectra obtained for a solid-supported lipid bilayer containing a 1:1 mixture of POPC and SM (panels A and D, curve 1) and for the incorporation of the agonist (DPDPE)-bound hDOR (~10 nM, final concentration in the sample cell) into the lipid bilayer (panels A and D, curve 2). Spectra were obtained with 543.5 nm (green) exciting light using either p (panels A−C)- or s-polarized light (panels D−F). Experimental PWR spectra and simulation of the POPC/SM (1:1) bilayer (panels B and E), and upon incorporation of hDOR into the bilayer (panels C and F), are shown. In panels B, C, E, and F, the solid curves containing the empty circles show the experimental spectra and the simulated spectra; the solid curves with the filled symbols represent the deconvoluted single-lipid component spectra for POPC (●) and SM (▲) obtained from the simulated fits. The simulated fit to the experimental spectra is the result of an appropriately weighted sum of the component curves.

mixture. As mentioned above, various spectroscopic studies have shown that phase separation can occur in binary lipid mixtures composed of lipids that have different phase transition temperatures. This process occurs spontaneously and requires only lipid−lipid interactions leading to the formation of microdomains. These are characterized by tightly packed lipids with limited lateral mobility that coexist with a liquid-disordered phase in which lipids are more fluid and with a higher degree of lateral mobility (*32*−*34*). As discussed above, the analysis of this type of PWR spectrum requires the deconvolution of the experimental curves into single-resonance spectra. Examples of such deconvolution are shown in panels B and E of Figure 1. The structural parameters of the microdomains obtained from these simulations, averaged for three separate experiments performed with POPC/SM (1:1) bilayers, were as follows. For the lower-angle component, a thickness of 5.4 ± 0.1 nm and a surface area per molecule of 0.49 ± 0.01 nm^2 were obtained, whereas for the higher-angle component, a thickness of 6.0 ± 0.1 nm and a surface area per molecule of 0.41 ± 0.01 nm^2 were obtained. Thus, the latter component is thicker and more densely packed than the former. These values can be compared with a thickness of 5.4 nm and a surface area per molecule of 0.48 nm^2 for a pure POPC bilayer, and a thickness of 6.1 nm and a surface area per molecule of 0.39 nm^2 for a pure SM bilayer (*24*), clearly indicating that the lower-angle component can be attributed to the POPC-rich phase and the higher-angle component to the SM-rich phase, as previously concluded.

The size of the microdomains can be evaluated from the lateral resolution of the PWR sensor used in this work. In general, the lateral resolution size of optically homogeneous areas in a sample, as detected by PWR spectroscopy, is in the micrometer range. The specific value will depend on the properties of the sensor that produces the surface-bound waves. In this context, one of the most important characteristics of such surface plasmon waves is that they propagate along a lossy interface, which results in a finite propagation length. A qualitative explanation of the relationship between the propagation length of the surface plasmon wave and the lateral resolution is based on the fact that the resonance will reflect the overall effective index of refraction integrated over the evanescent field. Therefore, if the surface architecture features are comparable to or smaller than the propagation length, one will see distinct resonances coming from such features. On the other hand, if the surface features are much smaller than the propagation length, then the optical refractive index will be averaged, resulting in one resonance with average values of the optical parameters. Furthermore, scattering effects will occur, resulting in significant broadening of the resonance. The PWR sensor employed in this work creates surface-bound waves with a propagation length of ~70 μm for green light (λ = 543.5 nm) and 350 μm for red light (λ = 632.8 nm) excitation. We estimate from this that the smallest size of microdomains that can be observed with this sensor will be ~20 μm (measured with green light). However, as the data demonstrate, the resonances obtained with the two microdomains are reasonably well separated, clearly indicating that the microdomain size observed in this work is significantly larger than 20 μm. Furthermore, we have been able to observe good separation between the two resonances using red light excitation (data not shown), which indicates that the microdomain size is probably in the range of 100−300 μm.

Insertion of the agonist-bound hDOR resulted in the spectra shown in the curves labeled 2 in Figure 1 (panels A and D). As can be seen from these spectra, incorporation of the protein influenced both the main maximum and the shoulder in both p- and s-polarizations, thereby changing the overall shape of the spectrum. Such spectral modifications are due both to mass density changes and to structural alterations of the proteolipid membrane. Larger shifts were obtained for the SM-rich than for the PC-rich domain upon incorporation of the receptor agonist into the bilayer. This can be more easily observed in the case of the s-polarization spectra (panel D), which are more sensitive to lateral lipid and protein segregation.

To quantify these changes, it is again necessary to deconvolute the complex experimental spectrum into single-component spectra corresponding to the two lipid microdomains that exist within the bilayer (i.e., POPC-rich and SM-rich). From these component spectra, it is then possible to calculate the mass and anisotropy changes that occur as a consequence of incorporating various liganded forms of the receptor into the microdomains. It is important to note that these studies are primarily focused on the distribution of the receptor within the bilayer, without evaluating the structural consequences of either receptor insertion or ligand binding. Because of this, we will not consider refractive index anisotropy in our discussion.

The evaluation of protein distribution within the bilayer is complicated by the fact that the amount of protein incorporated varied somewhat in individual experiments. Therefore, it is necessary to normalize the mass changes. This can be done by taking the difference between the mass changes in the two microdomains and dividing by the total mass changes in both domains, according to the following equation:

$$\Delta m^{SM} - \Delta m^{PC}/\Delta m^{PC} + \Delta m^{SM} \quad (1)$$

where $\Delta m^{SM} = m^{SM}_{(BLM+protein)} - m^{SM}_{(BLM)}$ and $\Delta m^{PC} = m^{PC}_{(BLM+protein)} - m^{PC}_{(BLM)}$. In this equation, the subscripts (BLM) and (BLM+protein) denote the total mass in each microdomain before and after protein incorporation, respectively. In this way, one is able to calculate a normalized protein redistribution, which quantifies the redistribution of the protein between the microdomains calculated per unit total mass change. Note that that such a definition of normalized protein redistribution indicates that three characteristic types of protein mass changes can occur. First, when $\Delta m^{SM} = \Delta m^{PC}$, there is no difference between incorporation into the microdomains and the result of eq 1 is zero. Second, if $\Delta m^{SM} > \Delta m^{PC}$, then more hDOR is incorporated into the SM-rich phase than into the POPC-rich phase and eq 1 yields a positive value. Third, if $\Delta m^{SM} < \Delta m^{PC}$, eq 1 yields a negative value, meaning more protein is inserted into the POPC-rich phase than into the SM-rich phase. The magnitudes of the values allow comparison of the extent of mass redistribution.

Table 1 shows the normalized protein redistribution values calculated for the agonist-bound receptor from the simulations given in Figure 1 (panels B, C, E, and F). As can be seen from these values, the incorporation of the agonist-bound receptor yields a positive value, indicating that the receptor prefers the SM-rich environment over the POPC-rich microdomain. It should be pointed out that studies performed with another delta opioid agonist, SNC80, also gave similar results, with a preferential partitioning of the receptor into the SM-rich phase (data not shown).

Table 1: Normalized Protein Redistribution between SM and POPC Microdomains for the hDOR Incorporated into a Lipid Membrane Formed from a 1:1 Mixture of POPC and SM

receptor	normalized protein redistribution factor
with DPDPE	0.26
no ligand	−0.19
with NTI	0.12

Previous studies have been directed toward investigating the effect of an agonist on the partitioning of receptors between microdomains (*9*, *10*), and the reported results were very diverse. Thus, some receptors such as the β_2-adrenergic (*11*) and the adenosine A_1 (*12*) receptors were found to move out of microdomains upon agonist activation, whereas others such as the angiotensin II type 1 receptor (*13*), the m2 muscarinic cholinergic receptor (*14*), and bradykinin 1 and 2 receptors (*15*−*17*) were found to move into microdomains upon agonist treatment. The localization of others, such as rhodopsin (*35*) and the β_1-adrenergic receptor (*11*), was unaffected by activation. Since these studies were performed with different techniques and were not performed with model membranes, it is difficult to provide a direct correlation with our experiments. Inasmuch as different results were obtained with receptors belonging to the same GPCR class, it seems that the response to agonist in term of receptor partitioning between domains is not related to the GPCR class to which the receptor belongs. The sorting behavior observed by the different receptors upon agonist stimulation in whole cell studies may involve the initiation of the signaling response by the differential partitioning of several elements of the signaling cascade in the domains, or it could be related to the mechanism of desensitization and internalization observed in most GPCRs after agonist treatment. To our knowledge, the studies presented here are the first ones with the delta opioid system, although studies have been performed with the mu opioid receptor in which agonist treatment was found to lead to a decrease in the diffusion coefficient of this receptor with colocalization in clathrin-rich regions (L. Salomé, personal communication).

As extensive literature has shown that detergents affect the existence of domains in lipid bilayers, and detergent was included in the solubilized receptor solution that was added to the system, a control experiment was performed in which similar amounts of octyl glucoside were added to the POPC/SM (1:1) bilayer in the absence of the receptor. No spectral changes were observed upon the addition of octyl glucoside at concentrations (0.5−1 mM) comparable to the ones used in the experiment with the receptor (data not shown). We thus conclude that detergent effects on the spectra shown in Figure 1 (as well as in the subsequent experiments) were absent.

Incorporation of the Unliganded hDOR in a POPC/SM (1:1) Bilayer. Panels A and B of Figure 2 show PWR spectra obtained with a POPC/SM (1:1) lipid membrane in the absence of incorporated hDOR, with overlapping spectra due to the two types of microdomains discussed above, before (curve 1) and after (curve 2) incorporation of the unliganded receptor. A qualitative comparison of these results with those

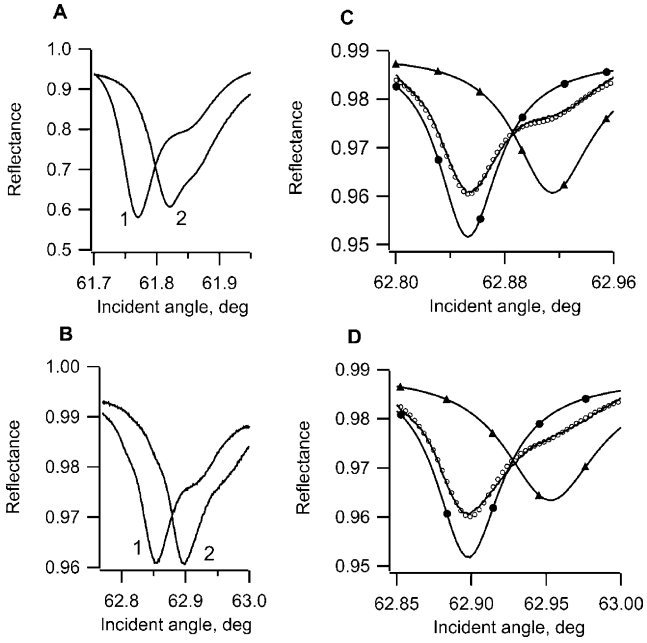

FIGURE 2: PWR spectra obtained for a solid-supported lipid bilayer containing a 1:1 mixture of POPC and SM (panels A and B, curve 1) and for the incorporation of the unliganded hDOR into the lipid bilayer (~10 nM, final concentration in the sample cell) (panels A and B, curve 2), obtained with 543.5 nm (green) exciting light using either p (panels A and C)- or s-polarized light (panels B and D). Panels C and D represent the simulation results for the incorporated receptor, as described in the legend of Figure 1, with the difference being that the receptor is now unliganded.

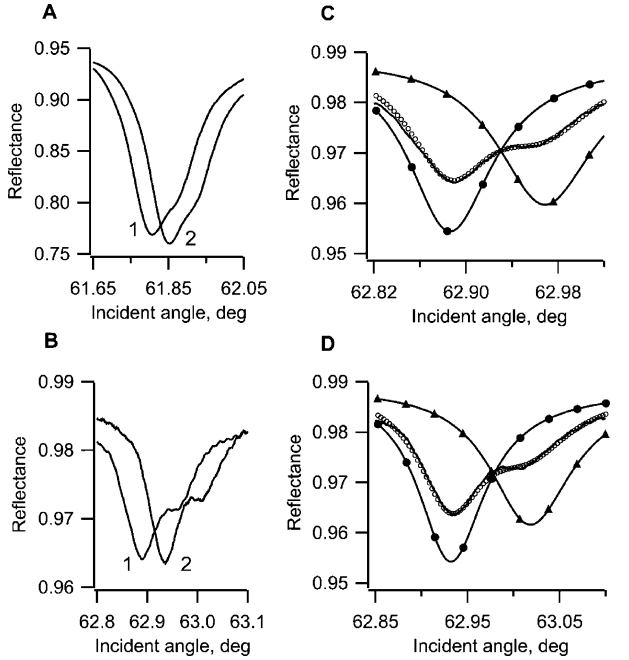

FIGURE 3: PWR spectra obtained for the supported lipid bilayer containing a 1:1 mixture of POPC and SM (panels A and B, curve 1) and for the incorporation of the antagonist (NTI)-bound hDOR into the lipid bilayer (panels A and B, curve 2) obtained with 543.5 nm (green) exciting light using either p (panels A and C)- or s-polarized light (panels B and D). Panels C and D represent the simulation results for the incorporated receptor, as described in the legend of Figure 1, with the difference being that the receptor is now bound to the antagonist, naltrindole.

presented in panels A and D of Figure 1 shows significant differences in the spectral characteristics of the initial bilayer spectra. These differences in spectral shape can be explained by different contributions of each type of microdomain to the experimental spectrum, caused by the heterogeneous nature of the surface area of the bilayer probed by the exciting light. This heterogeneity varies from experiment to experiment. However, as we have shown previously (*24*), this does not affect the properties of the individual microdomains obtained by the deconvolution process.

There are also significant differences between Figures 1 and 2 with regard to the shift of the spectra as a result of receptor incorporation. As noted above, in the case of the agonist-bound receptor, the higher-angle shoulder (i.e., the SM-rich phase) is shifted more than the main portion of the spectrum (i.e., the PC-rich phase) toward larger angles. In the case of unliganded receptor incorporation, the opposite is true; i.e., the main spectrum is shifted more than the shoulder toward the higher angles. This observation is clearly supported by the quantitative analysis of the normalized protein redistribution presented in Table 1. This demonstrates that more receptor is inserted into the PC-rich phase than into the SM-rich microdomain (i.e., the value is negative).

Incorporation of the Antagonist-Bound (naltrindole) hDOR into a POPC/SM (1:1) Bilayer. As can be seen from both Figure 3 and Table 1, the incorporation of hDOR bound to the antagonist, naltrindole, leads to partitioning of the receptor in larger amounts into the SM-rich domain than into the PC-rich phase. However, the difference between incorporation of the protein into the two domains is smaller than in the case with the agonist-bound receptor (i.e., a smaller positive value is obtained; cf. Table 1). Note also that the spectral properties of the bilayer are again different from those shown in Figures 1 and 2, for the reason noted above.

Previous studies performed in our laboratory using PWR point to the fact that the opioid receptor adopts different conformations upon binding of different classes of ligands (*22*). The different partitioning observed between the domains for the unliganded and for the agonist- versus antagonist-bound receptor may therefore be related to the different structures induced by the ligands relative to the unliganded protein, where certain conformations may be favored in one type of lipid microdomain over others. PWR and other studies involving the delta opioid receptor (*22*) and rhodopsin, the GPCR prototype, have shown that the receptor is elongated upon agonist and light activation (*36*). As demonstrated by our PWR results, as well as by AFM studies (*37*, *38*), the SM-rich domain is thicker than the PC-rich domain, as a consequence of the presence of longer, largely saturated acyl chains. Since the agonist-activated receptor is more elongated than the unliganded or antagonist-bound receptor, implying a larger hydrophobic thickness, we hypothesize that hydrophobic matching between the receptor and the bilayer provides the basis for the different receptor partitioning in each case. Thus, the unliganded receptor, having a less elongated structure, would prefer the PC-rich microenvironment with its shorter hydrophobic length. Lipid mismatch and consequent lateral lipid phase separation have been observed as a result of varying the chain length of lipids, and the concept of hydrophobic mismatching has also been applied to lipid−protein interactions (*20*, *39*−*42*). This hypothesis can also explain the larger amounts of antagonist-bound receptor incorporated into the SM-rich phase as compared to the unliganded receptor. As we have demon-

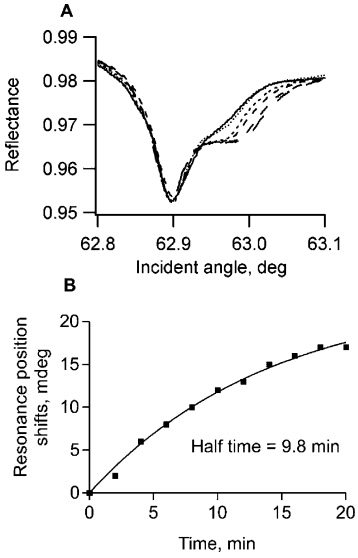

FIGURE 4: Time evolution of PWR spectra, obtained with s-polarized light, upon addition of an agonist (DPDPE) to the receptor when incorporated into a POPC/SM (1:1) lipid bilayer (A). With respect to the right shoulder, from left to right the spectra represent increasing time intervals: (—) 0, (•••) 2, (- - -) 6, (— — —) 8, (— — —) 16, and (— — —) 20 min. Panel B represents a plot of the spectral shifts obtained in panel A as a function of time. The solid curve is a fit of the data to a single exponential using the equation $Y = Y_{max}[1 - \exp(-kX)]$, where Y_{max} is the maximal rate obtained, k is the first-order rate constant, and the half-time is 0.693/k. The fit was obtained with GraphPad Prism (San Diego, CA).

strated previously (*22*), binding of an antagonist results in receptor conformation changes leading to a more parallel orientation of the transmembrane helices (i.e., a higher degree of refractive index anisotropy). This will also increase the hydrophobic length of the protein (although perhaps less so than protein elongation), which would again lead to a more preferable redistribution of the antagonist-bound receptor to the SM-rich microdomain. It should be pointed out, however, that hydrophobic matching is not the only possible contribution to the results. This is discussed in more detail below.

Addition of an Agonist to the Unliganded hDOR Reconstituted into a POPC/SM (1:1) Bilayer. We have also incorporated the receptor with no ligand bound into the bilayer and monitored spectral changes occurring upon addition of the DPDPE agonist (similar results were obtained with SNC80) to the proteolipid system (Figure 4A). The addition of agonist to the proteolipid system leads to enrichment of receptor in the SM-rich domain, as noted by the larger spectral changes observed in the part of the spectra attributed to the SM-rich domain (i.e., the larger angle side of the spectra). As can be seen by comparison of these spectra to those shown in Figure 1D, the distribution of protein was approximately the same regardless of whether the ligand was bound before or after incorporation of the receptor into the bilayer. By monitoring the spectral changes as a function of time, we were able to determine the kinetics of the movement of the receptor from the PC-rich to the SM-rich domain (Figure 4B), which is shown to occur with a half-time of approximately 10 min. We believe that the slow kinetics observed may partly be a consequence of the shearing forces in the receptor and lipids due to the interaction with the silica surface of the sensor and thus may not compare well with results observed in vivo. It is also possible that these kinetics

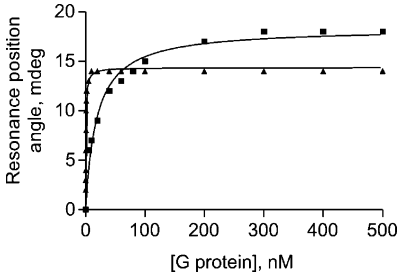

FIGURE 5: Binding curves obtained for interaction of the G-protein ($G_{i\alpha2}$-$\beta\gamma$) with the DPDPE-liganded hDOR when reconstituted into a POPC/SM (1:1) bilayer obtained using p (■)- and s-polarized light (▲). Solid curves correspond to hyperbolic fits to the data performed using the equation that describes the 1:1 binding of a ligand to a receptor, $Y = (B_{max}X)/(K_D + X)$, where B_{max} represents the maximum concentration bound and K_D is the concentration of ligand required to reach half-maximal binding. Dissociation constant (K_D) values are given in Table 2.

Table 2: Interaction of the G-Protein ($G_{i\alpha2} + \beta\gamma$) with the DPDPE hDOR and Interaction of GTPγS with the Ligand—Receptor—G-Protein Complex[a]

	K_D (G-protein) (nM)		K_D (GTPγS) (nM)	
	p-polar.	s-polar.	p-polar.	s-polar.
POPC/SM (1:1), POPC-rich	6[b]	19	12[b]	11
POPC/SM (1:1), SM-rich		0.6		10
POPC	32		11	
egg PC/POPG (75:25)	7		9	

[a] K_D values were obtained from plotting the resonance minimum position for the PWR spectra as a function of G-protein concentration and fitting to the following hyperbolic function that describes the binding of a ligand to a receptor: $Y = (B_{max}X)/(K_D + X)$. B_{max} represents the maximum concentration bound, and K_D is the concentration of ligand required to reach half-maximal binding. [b] Because of the difficulty in separating the spectral changes upon interaction of the G-protein with the PC-rich and SM-rich domains for the p-polarized spectra, only one value is presented that corresponds to the shift obtained in the major minimum in the spectra (attributed predominantly to the PC-rich phase).

may be influenced by the relatively large microdomain size in these bilayers. Furthermore, we cannot determine if the receptor is actually moving into an SM-rich microdomain, or whether the elongated receptor is recruiting SM molecules into its immediate environment; both processes are possibly occurring.

Interaction of the G-Protein with a hDOR Agonist Inserted into a POPC/SM (1:1) Bilayer. Previous studies performed in our laboratory have investigated G-protein—receptor interaction using this same PWR methodology, where affinities were obtained for different ligands bound to the receptor and different subtypes of G-proteins (*23*). Using the information obtained from these studies, we have investigated the effect of domain formation on the affinity of the $G_{i\alpha2}$-$\beta\gamma$ subtype (the α-subunit with the highest affinity for the DPDPE hDOR) for the agonist-activated hDOR. As demonstrated in Figure 5 and Table 2, this G-protein subtype has a much higher affinity for the DPDPE receptor inserted into the SM-rich domain ($K_D = 0.6$ nM) than the one present in the PC-rich domain ($K_D = 19$ nM). As can be seen in Table 2, the affinity of the $G_{i\alpha2}$-$\beta\gamma$ subtype for the agonist-bound receptor is very much dependent on the lipid environment surrounding the receptor, having the greatest affinity for the receptor in an SM-rich domain and the least for a receptor in a pure POPC bilayer. Note also that the affinity is higher in the POPC-rich microdomain than in the pure

POPC bilayer. Thus, the presence of a small amount of SM in this domain facilitates G-protein binding. The affinity of GTPγS for the ligand−receptor−G-protein complex was investigated by a strategy previously used (*23*), but no effects of lipid microenvironment were observed here (Table 2). Thus, as we have shown previously for the effects of ligand binding (*23*), G-protein binding and activation are influenced differently by variations in the properties of the receptor caused by environmental effects. We conclude that it is the ability of the receptor to achieve a high-affinity G-protein conformational state that is being modulated by the microenvironment.

It is important to mention that a control experiment on the interaction of the G-protein with the POPC/SM (1:1) bilayer in the absence of receptor was performed by observing spectral changes upon incremental addition of G-protein. Very small shifts were observed for both polarizations (~5 mdeg) with the data following a straight-line relation, as usually observed for nonspecific interactions. Similar observations have been reported previously for the interaction of G-proteins with non-domain-forming bilayers (*23*).

Contrasting results have been found previously with regard to the partitioning of the G-protein in lipid domains. Some experiments have reported that G-proteins are enriched in lipid microdomains, including G_s, G_i, G_o, G_q, and transducin (*35*, *43*, *44*), and their localization was proposed to be a result of the α subunit acylation (*47*), whereas others have shown that the presence of microdomains does not affect membrane partitioning of G-proteins (*46*). The experiments described here show that the affinity of G-proteins for each domain is different only when the receptor is inserted into those domains. Thus, the differential partitioning of G-proteins into each domain, in our studies, seems to be promoted by the receptor itself and not by a preferential interaction of the G-protein with the microdomain. A possible mechanism is that the receptor adopts a slightly different conformation in each domain that may be more or less favorable for G-protein interaction.

CONCLUSIONS

The results obtained in these studies have confirmed earlier experimental evidence (*2*, *24*) which showed that spontaneous lateral segregation of lipids into microdomains occurs in solid-supported bilayers containing binary mixtures of POPC and sphingomyelin. Such segregation produces regions within the bilayer whose different optical properties allow observation of separate resonances in a PWR experiment. Furthermore, in this work, we have demonstrated a differential partitioning of the hDOR, a G-protein-coupled receptor, between lipid microdomains that was highly dependent on the ligand-induced activation state of the receptor. These observations are consistent with earlier PWR results obtained with both rhodopsin (*47*) and the hDOR (*22*) using solid-supported membranes composed of single lipids that are known to form a laterally homogeneous type of planar bilayer. In these earlier experiments, it was demonstrated that the activation of both rhodopsin and the hDOR resulted in the formation of a new protein conformational state that induced structural alterations of the lipid microenvironment around the receptor, creating what may be considered a new microdomain within the original planar lipid bilayer structure. Thus, activation by agonist binding in the case of the hDOR, or by light in the case of rhodopsin, produced an elongation of the receptor molecule (i.e., an increase in the receptor dimension along its vertical axis), which was accompanied by movement of lipid molecules that caused both an overall increase in the degree of orientational order localized around the receptor (i.e., an increase in refractive index anisotropy) and an increase in the negative curvature of the lipid membrane surface in contact with the receptor. In contrast, the binding of the antagonist to the hDOR resulted in only an increase in the refractive index anisotropy, which implies localized alterations occurring within the receptor molecule that are restricted to the transmembrane helices and to the lipid hydrocarbon chain orientation, without involving any protein elongation.

This work has further proven the validity of such models by studies of receptor interaction with lipid microdomains of different structure and thickness created within a POPC/SM membrane. These results have shown that the sorting of the hDOR into each membrane domain was highly dependent on the type of ligand that was bound. Thus, the agonist-activated receptor had a higher affinity for the thicker and more ordered SM-rich microdomain (*48*) than either the inactive (unliganded) or antagonist-activated protein. Furthermore, the binding of an agonist to an unliganded hDOR molecule in the bilayer produced receptor trafficking from the PC-rich to the SM-rich domain. This is consistent with the elongation of the receptor and the anisotropy increase postulated in the earlier work. The results also indicate that the new receptor conformation requires rearrangement of the lipid microenvironment around such an activated receptor. An appropriate microenvironment can be induced by the new receptor structure, as we have demonstrated in the earlier studies (*22*), or the activated receptor can either move into another membrane phase or reorganize the microenvironment around it, to better accommodate its structure, as we have shown in the work presented here.

There is, however, still an open question; i.e., what is the driving force for these two pathways of creating new lipid microenvironments after receptor activation? The obvious answer seems to be hydrophobic matching. However, there are other factors that may also play a role. Among these is the effect of alteration of the mechanical properties of the lipid membrane on the functioning of the receptor. One would expect that the changes in the lipid microenvironment result in alteration of the mechanical forces within the bilayer such as transbilayer pressure. It has been clearly demonstrated with some types of ion channels that the lateral or transmembrane pressure profile of the bilayer can control the conformational equilibrium of the protein (*49*). In this context, it is important to note that in this work we have shown that the affinity of the G-protein for the agonist-bound hDOR was modulated by the receptor location either inside or outside the SM-rich region, suggesting that this microenvironment promotes receptor conformations that are favorable for G-protein interaction. This is an example of the more general question of the role of lipid membrane structural and mechanical properties in membrane protein function that requires further study.

The techniques available at present for studying lipid microdomains are rife with methodological pitfalls and limitations, and many studies utilize fairly indirect approaches, such as cholesterol depletion, which, if not carefully employed, may lead to mistaken conclusions (*10*). Although in vivo studies are exceptionally important, their understanding is complicated by the presence of a large variety of microdomains in the bilayer and by the existence of a cytoskeleton and other structuring organelles, which may also lead to protein compartmentalization, as well as by the presence of several proteins (e.g., receptors, caveolin, G-proteins, etc.), which may also be involved in the receptor partitioning and trafficking. In this respect, the use of a model lipid membrane may be advantageous, allowing one to investigate a large range of lipid bilayer compositions in the presence or absence of particular proteins, thereby permitting one to focus on individual aspects of the signaling cascade. PWR technology, by allowing one to perform the experiments described above in real time under physiological conditions of pH, concentration, etc., should be of considerable use in the ongoing process of understanding the role of microdomains in signal transduction. It is important to note, however, that the present model membrane system differs from biological membranes in its lack of transverse lipid compositional asymmetry, and in the bidirectional insertion of the receptor (*30*). How this might influence the properties described here is unclear at present.

We should also note that these experiments were performed without the inclusion of cholesterol in the bilayers. Although this lipid clearly plays a role in microdomain formation in bilayers (both in vivo and in vitro), the precise structural basis for this is at present unclear (*50*). We have indeed carried out PWR experiments with ternary lipid mixtures containing cholesterol and have found that the results are qualitatively similar to those we obtained with the binary systems (data not shown). Thus, it appears that the effects of cholesterol are subtle and will require a good deal of work to sort out. We plan to do this in future experiments.

ACKNOWLEDGMENT

We acknowledge the laboratory of Dr. H. I. Yamamura for providing us with the CHO cell line expressing the hDOR.

REFERENCES

1. Singer, S. J., and Nicolson, G. L. (1972) The fluid mosaic model of the structure of cell membranes, *Science 175*, 720−731.
2. Simons, K., and Vaz, W. L. C. (2004) Model systems, lipid rafts, and cell membranes, *Annu. Rev. Biophys. Biomol. Struct. 33*, 269−295.
3. Simons, K., and Ikonen, E. (1997) Functional rafts in cell membranes, *Nature 387*, 569−572.
4. Brown, D. A., and London, E. (2000) Structure and function of sphingolipid- and cholesterol-rich membrane rafts, *J. Biol. Chem. 275*, 17221−17224.
5. Simons, K., and Toomre, D. (2000) Lipid rafts and signal transduction, *Nat. Rev. Mol. Cell Biol. 1*, 31−41.
6. Navratil, A. M., Bliss, S. P., Berghorn, K. A., Haughian, J. M., Farmerie, T. A., Graham, J. K., Clay, C. M., and Roberson, M. S. (2003) Constitutive localization of the gonadotropin-releasing hormone (GnRH) to low-density membrane microdomains is necessary for GnRH signaling to ERK, *J. Biol. Chem. 278*, 31593−31602.
7. Gimpl, G., and Faahrenholz, F. (1997) Human oxytocin receptors in cholesterol-rich vs cholesterol-poor microdomains of the plasma membrane, *Biochemistry 36*, 10959−10974.
8. Guzzi, F., Zanchetta, D., Cassoni, P., Guzzi, V., Francolini, M., Parenti, M., and Chini, B. (2002) Localization of the human oxytocin receptor in caveolin-1 enriched domains turns the receptor-mediated inhibition of cell growth into a proliferative response, *Oncogene 21*, 1658−1667.
9. Chini, B., and Parenti, M. (2004) G-protein coupled receptors in lipid rafts and caveolae: How, when and why do they go there?, *J. Mol. Endocrinol. 32*, 325−338.
10. Pike, L. J. (2003) Lipid rafts: Bringing order to chaos, *J. Lipid Res. 44*, 655−667.
11. Dessy, C., Kelly, R. A., Balligand, J.-L., and Feron, O. (2000) Dynamin mediates caveolar sequestration of muscarinic cholinergic receptors and alteration in NO signaling, *EMBO J. 19*, 4272−4280.
12. Lasley, R. D., Narayan, P., Uittenbogaard, A., and Smart, E. J. (2000) Activated cardiac adenosine A_1 receptors translocate out of caveolae, *J. Biol. Chem. 275*, 4417−4421.
13. Ishizaka, N., Griendling, K., Lassegue, B., and Alexander, R. W. (1998) Angiotensin II type I receptor: Relationship with caveolae and caveolin after initial agonist stimulation, *Hypertension 32*, 459−466.
14. Feron, O., Smith, T. W., Michel, T., and Kelly, R. A. (1997) Dynamic targeting of the agonist-stimulated m2 muscarinic acetylcholine receptor to caveolae in cardiac myocytes, *J. Biol. Chem. 272*, 17744−17748.
15. de Weerd, W. F. C., and Leeb-Lundberg, L. M. F. (1997) Bradykinin sequesters B2 bradykinin receptors and the receptor-coupled Gα subunits Gαq and Gαi in caveolae in DDT1 MF-2 smooth muscle cells, *J. Biol. Chem. 272*, 17858−17866.
16. Haaseman, M., Cartaud, J., Muller-Esterl, W., and Dunia, I. (1998) Agonist-induced redistribution of bradykinin B2 receptor in caveolae, *J. Cell Sci. 111*, 917−928.
17. Sabourin, T., Bastien, L., Bachvarov, D. R., and Marceau, F. (2002) Agonist-induced translocation of the kinin B_1 receptor to caveolae-related rafts, *Mol. Pharmacol. 61*, 546−553.
18. Chun, M., Liyanage, U. K., Lisanti, M. P., and Lodish, H. F. (1994) Signal transduction of a G-protein coupled receptor in caveolae: Colocalization of endothelin and its receptor with caveolin, *Proc. Natl. Acad. Sci. U.S.A. 91*, 11728−11732.
19. Bretscher, M. S., and Munro, S. (1993) Cholesterol and the Golgi apparatus, *Science 261*, 1280−1281.
20. Killian, J. A. (1998) Hydrophobic mismatch between proteins and lipids in membranes, *Biochim. Biophys. Acta 1376*, 401−416.
21. Quock, R. M., Burkey, T. H., Varga, E., Hosohata, K., Cowell, S. M., Slate, C. A., Ehlert, F. J., Roeske, W. R., and Yamamura, H. I. (1999) The δ-opioid receptor: Molecular pharmacology, signal transduction and the determination of drug efficacy, *Pharmacol. Rev. 51*, 503−532.
22. Salamon, Z., Cowell, S., Varga, E., Yamamura, H. I., Hruby, V. J., and Tollin, G. (2000) Plasmon resonance studies of agonist/antagonist binding to the human δ-opioid receptor: New structural insights into receptor−ligand interactions, *Biophys. J. 79*, 2463−2474.
23. Alves, I. D., Ciano, K. A., Boguslavski, V., Varga, E., Salamon, Z., Yamamura, H. I., Hruby, V. J., and Tollin, G. (2004) Selectivity, cooperativity and reciprocity in the interactions between the δ-opioid receptor, its ligands, and G-proteins, *J. Biol. Chem. 279*, 44673−44682.
24. Salamon, Z., Devanathan, S., Alves, I. D., and Tollin, G. (2005) Plasmon-waveguide resonance studies of lateral segregation of lipids and proteins into microdomains (rafts) in solid-supported bilayers, *J. Biol. Chem. 280*, 11175−11184.
25. Salamon, Z., Brown, M. F., and Tollin, G. (1999) Plasmon resonance spectroscopy: Probing interactions within membranes, *Trends Biochem. Sci. 24*, 213−219.
26. Salamon, Z., and Tollin, G. (2001) Plasmon resonance spectroscopy: Probing molecular interactions at surfaces and interfaces, *Spectroscopy 15*, 161−175.
27. Tollin, G., Salamon, Z., and Hruby, V. J. (2003) Techniques: Plasmon-waveguide resonance (PWR) spectroscopy as a tool to study ligand-GPCR interactions, *Trends Pharmacol. Sci. 24*, 655−659.
28. Salamon, Z., Macleod, H. A., and Tollin, G. (1997) Coupled plasmon-waveguide resonators: A new spectroscopic tool for probing proteolipid film structure and properties, *Biophys. J. 73*, 2791−2797.

29. Okura, T., Cowell, S. M., Varga, E., Burkey, T. H., Roeske, W. R., Hruby, V. J., and Yamamura, H. I. (2000) Differential down-regulation of the human delta-opioid receptor by SNC80 and [DPen (2), DPen (5)]enkephalin, *Eur. J. Pharmacol. 387*, R11−R13.
30. Alves, I., Varga, E., Salamon, Z., Yamamura, H. I., Tollin, G., and Hruby, V. J. (2003) Direct observation of G-protein binding to the human δ-opioid receptor using plasmon-waveguide resonance spectroscopy, *J. Biol. Chem. 278*, 48890−48897.
31. Mueller, P., Rudin, D. O., Tien, H. T., and Wescott, W. C. (1962) Reconstitution of cell membrane structure in vitro and its transformation into an excitable system, *Nature 194*, 979−980.
32. Rinia, H. A., Snel, M. M., van der Eerden, J. P., and de Kruijff, B. (2001) Visualizing detergent resistant domains in model membranes with atomic force microscopy, *FEBS Lett. 501*, 92−96.
33. Saslowsky, D. E., Lawrence, J., Ren, X., Brown, D. A., Henderson, R. M., and Edwardson, J. M. (2002) Placental alkaline phosphatase is efficiently targeted to rafts in supported lipid bilayers, *J. Biol. Chem. 277*, 26966−26970.
34. Almeida, R. F. M., Fedorov, A., and Prieto, M. (2003) Sphingomyelin/phosphatidylcholine/cholesterol phase diagram: Boundaries and composition of lipid rafts, *Biophys. J. 85*, 2406−2416.
35. Seno, K., Kishimoto, M., Abe, M., Higuchi, Y., Mieda, M., Owada, Y., Yoshiyama, W., Liu, H., and Hayashi, F. (2001) Light- and guanosine 5′-3-O-(thio)triphosphate-sensitive localization of a G protein and its effector in detergent-resistant membrane rafts in rod photoreceptor outer segments, *J. Biol. Chem. 276*, 20813−20816.
36. Farrens, D. L., Altenbach, C., Yang, K., Hubbell, W. L., and Khorana, H. G. (1996) Requirement of rigid body motion of transmembrane helices for light activation of rhodopsin, *Science 274*, 768−770.
37. Milhiet, P. E., Giocondi, M.-C., and Le Grimellec, C. (2002) Cholesterol is not crucial for the existence of microdomains in kidney brush-border membrane models, *J. Biol. Chem. 277*, 875−878.
38. Muresan, A. S., Diamant, H., and Lee, K. Y. C. (2001) Effect of temperature and composition on the formation of nanoscale components in phospholipid membranes, *J. Am. Chem. Soc. 123*, 6951−6952.
39. Fattal, D. R., and Ben-Shaul, A. (1993) A molecular model for lipid−protein interactions in membranes: The role of hydrophobic mismatch, *Biophys. J. 65*, 1795−1809.
40. Ren, J., Lew, S., Wang, J., and London, E. (1999) Control of the transmembrane orientation and interhelical interactions within membranes by hydrophobic helix length, *Biochemistry 38*, 5905−5912.
41. Harroun, T. A., Heller, W. T., Weiss, T. M., Yang, L., and Huang, H. W. (1999) Experimental evidence for hydrophobic matching and membrane-mediated interactions in lipid bilayers containing gramicidin, *Biophys. J. 76*, 937−945.
42. McIntosh, T. J., Vidal, A., and Simon, S. A. (2003) Sorting of lipids and transmembrane proteins between detergent-soluble bilayers and detergent-resistant rafts, *Biophys. J. 85*, 1656−1666.
43. Huang, C., Hepler, J. R., Chen, L. T., Gilman, A. G., Anderson, R. G., and Mumby, S. M. (1997) Organization of G proteins and adenylyl cyclase at the plasma membrane, *Mol. Biol. Cell 8*, 2365−2378.
44. Oh, P., and Schnitzer, J. E. (2001) Segregation of heterotrimeric G proteins in cell surface microdomains. G_q binds caveolin to concentrate in caveolae, whereas G_i and G_s target lipid rafts by default, *Mol. Biol. Cell 12*, 685−698.
45. Moffett, S., Brown, D. A., and Linder, M. E. (2000) Light-dependent targeting of G proteins into rafts, *J. Biol. Chem. 275*, 2191−2198.
46. Philip, F., and Scarlata, S. (2004) Influence of membrane components in the binding of proteins to membrane surfaces, *Biochemistry 43*, 11691−11700.
47. Salamon, Z., Wang, Y., Brown, M. F., Macleod, H. A., and Tollin, G. (1994) Conformational changes in rhodopsin probed by surface plasmon resonance spectroscopy, *Biochemistry 33*, 13706−13711.
48. Sprong, H., van der Sluijs, H. P., and van Meer, G. (2001) How proteins move lipids and lipids move proteins, *Nat. Rev. Mol. Cell Biol. 2*, 504−513.
49. Abe, F., and Iida, H. (2003) Pressure-induced differential regulation of the two tryptophan permeases Tat 1 and Tat 2 by ubiquitin ligase Rsp5 and its binding proteins, Bul 1 and Bul 2, *Mol. Cell. Biol. 23*, 7566−7584.
50. Crane, J. M., and Tamm, L. (2004) Role of cholesterol in the formation and nature of lipid rafts in planar and spherical model membranes, *Biophys. J. 86*, 2965−2979.

BI050207A